

ORIGINAL ARTICLE

WEE1 accumulation and deregulation of S-phase proteins mediate MLN4924 potent inhibitory effect on Ewing sarcoma cells

C Mackintosh^{1,6}, DJ García-Domínguez^{1,6}, JL Ordóñez¹, A Ginel-Picardo², PG Smith³, MP Sacristán⁴ and E de Álava^{1,5}

Ewing sarcoma (ES) is an aggressive bone and soft tissue tumor of children and young adults in which finding effective new targeted therapies is imperative. Here, we report an in-depth preclinical study of the investigational cullin-RING ubiquitin ligase (CRL) inhibitor MLN4924 in ES, as we have recently demonstrated the implication of a CRL component in the ES pathogenesis. First, our results support a high sensitivity of ES cells to MLN4924 growth inhibition both *in vitro* (14 ES cell lines tested, median IC50 = 81 nM) and in tumor xenografts (tumor regression achieved with 60 mg/kg BID, subcutaneously, *n* = 9). Second, we report a dual mechanism of action of MLN4924 in ES cells: while a wide range of MLN4924 concentrations (~30–300 nM) trigger a G2 arrest that can only be rescued by WEE1 kinase inhibition or depletion, saturating doses of the drug (>300 nM) cause a delay in S-phase progression concomitant with unbalanced CDK2-Cyclin E and CDK2-Cyclin A relative levels (accumulation of the first and depletion of the latter). The aberrant presence of CDC6 in the nucleus at late S-phase cell cycle stage confirmed the loss of CDK2-Cyclin A-specific functions. Remarkably, other mechanisms explored (P27 accumulation and DNA damage signaling pathways) were found unable to explain MLN4924 effects, strengthening the specificity of our findings and suggesting the absence of functionality of some CRL substrates accumulated in response to MLN4924. This study renders a rationale for clinical trials and contributes molecular mechanisms for a better understanding of this promising antitumoral agent.

Oncogene advance online publication, 28 May 2012; doi:10.1038/onc.2012.153

Keywords: MLN4924; Ewing sarcoma; WEE1; cyclin A; cyclin E; P27

INTRODUCTION

Ewing sarcoma (ES) is an aggressive tumor that arises from the bone or soft tissue of children and young adults, being the second most frequent bone tumor at childhood.¹ Despite significant therapeutic advances in multimodal therapy, survival rates are still below 20% in patients with relapsed and/or disseminated disease.² Although several targeted therapies have been proposed based on preclinical studies, none has yet been agreed for the clinical routine, which makes this research an area of immediate concern.

We have recently shown that the genomic gain of an extra 1q chromosome copy strongly correlates with a poorer survival of ES patients.³ In this same study, overexpression of *CDT2*, a gene located at 1q32.3, was found as a major effector of this oncogenic copy number aberration. Given that *CDT2* is the main substrate receptor of the cullin-RING ubiquitin ligase (CRL) complex CUL4/DDB1, a rationale for a targeted therapy based on the inhibition of this CRL was proposed.

CRLs are a class of protein-ubiquitin ligases that target a wide range of proteins for degradation via proteasome 26S, being SCF (Skp, Cullin, F-box-containing complex) the best characterized CRL.⁴ Notwithstanding, there are dozens of different CRLs resulting from the combination of the diverse variants of each of the multiple molecular elements that constitute their structure (cullins 1 to 7, E3 ligases RBX1 and RNF7, several substrate

adapters and, specially, a plethora of different substrate receptors). Each possible CRL configuration targets a particular set of proteins,⁵ usually through the recognition of a phospho-degron motif, a signal that triggers the degradation process. This high complexity in structure and substrate recognition patterns probably reflects the fine regulation in time and space required for the proper development of the cellular functions regulated by CRLs. It is worth noting that CRLs are essential for the correct completion of every cell cycle stage, which makes them key regulators of this cellular process.⁶

MLN4924 is an investigational novel antitumoral agent that inhibits the Nedd8-activating enzyme UBA3, impairing the neddylation of the cullin component of CRLs, a process required for enabling the E3 ligase enzymatic activity that ultimately performs poly-ubiquitin binding to CRL substrates.^{7–8} By this means, MLN4924 inhibits CRL enzymatic activity, causing an increase in the protein levels of its substrates,⁹ many of which have been reported as potent tumor suppressors (among others P21, P27, IKB α and WEE1),^{10–13} while others have been described as oncogenes (among others CDC25A and Cyclin E).^{14–15}

Here, we report an in-depth preclinical evaluation of MLN4924 in ES. Our results show the potential high sensitivity of ES tumors to CRL inhibition and unveil a MLN4924 mechanism of action consisting of an induced G2 cell cycle arrest. Our data support

¹Molecular Pathology Program, IBSAL-Centro de Investigación del Cáncer-IBMCC (USAL-CSIC), Campus Miguel de Unamuno S/N, Salamanca, Spain; ²Laboratory 1, Centro de Investigación del Cáncer-IBMCC (USAL-CSIC), Campus Miguel de Unamuno S/N, Salamanca, Spain; ³Discovery, Millennium Pharmaceuticals, Inc., Cambridge, MA, USA; ⁴Department of Microbiology and Genetics, Centro de Investigación del Cáncer-IBMCC (USAL-CSIC), Campus Miguel de Unamuno S/N, Salamanca, Spain and ⁵Department of Pathology, IBSAL-University Hospital of Salamanca, Paseo San Vicente 58–182, Salamanca, Spain. Correspondence: Dr C Mackintosh, Molecular Pathology Program, IBSAL-Centro de Investigación del Cáncer-IBMCC (USAL-CSIC), Campus Miguel de Unamuno S/N, 37007 Salamanca, Spain or Dr E de Álava, Molecular Pathology Program, IBSAL-Centro de Investigación del Cáncer-IBMCC (USAL-CSIC), Campus Miguel de Unamuno S/N, 37007 Salamanca, Spain.

E-mail: cmackintosh@usal.es or edealava@usal.es

⁶These authors contributed equally to this work.

Received 5 December 2011; revised 21 February 2012; accepted 30 March 2012

a major role for WEE1 mediating this new molecular mechanism. In addition, MLN4924 saturating levels induced S-phase delay paralleled by depletion and loss of function of CDK2–Cyclin A complexes.

RESULTS

ES cell lines are highly sensitive to MLN4924

A total of 14 ES cell lines were treated with MLN4924 in order to estimate its ability to impair the *in vitro* growth of ES cell cultures (Table 1). The median IC50 (the concentration that reduces cell population by 50%) obtained (81 nM) is noticeably lower than that previously obtained for 10 cell lines belonging to 7 different tumor entities (200 nM)⁷ and similar to that of diffuse large B-cell lymphoma cell lines, which are the most sensitive to MLN4924 treatment as reported to date (76 nM).¹⁶ Interestingly, a recently published study has surveyed the *in vitro* sensitivity of a panel of pediatric cancer cell lines to MLN4924, finding ES cells to be the most sensitive ones to this compound, among those tested.¹⁷

No differences in IC50 owing to 1q copy number were observed (Figure 1a). Although we initially foresaw a higher sensitivity of 1q gain cells to CRL inhibition, this result broadens the potential application of MLN4924 to virtually all ES patients.

MLN4924 was also able to decrease *in vivo* growth of RDES xenograft tumors in mice at 30 mg/kg dosed twice daily (BID), whereas 60 mg/kg BID caused regression of the initial tumor mass (Figure 1b).

MLN4924 delays G2/M- and S-phase progression and induces apoptosis in ES cells

Flow cytometry analysis of DNA content evidenced a prominent increase in G2/M population 24 h after treatment with a broad range of MLN4924 concentrations (30–300 nM, equivalent to IC50–IC90 in most of the cell lines), while saturating doses elicited an accumulation of cells in S-phase (~300–1000 nM) together with the aforementioned G2/M peak (Figure 1c). The effect on G2/M ranged from a delay (Figures 1c, 2c) to a severe arrest (Figure 3d) depending on MLN4924 concentration. We will refer to it here as G2/M arrest to simplify the writing. The arrest was confirmed to persist after longer treatment periods (48 and 72 h, data not shown).

Induced apoptosis was detectable after 24 h of MLN4924 treatment, cleaved Caspase-3-positive population ranging from 4.7 to 10% at IC75 and from 17 to 31% at IC95 (Figure 1d). Combined flow cytometry analysis of propidium iodide and cleaved Caspase-3-labeled cells revealed a late S-G2 DNA content of apoptotic cells in RDES cell line, pointing to a common

mechanism underlying both S-G2 increase and cell death (Figure 1e).

Consistent with their similar sensitivity to MLN4924, 1q gain and 1q normal cell lines did not display any difference neither in cell cycle distribution profile nor in induced apoptosis in response to MLN4924, indicating a mechanism of action independent from 1q copy number (Figures 1c and d).

Protein levels of several regulators of the G2/M transition increase shortly after MLN4924 treatment and are stable after 24 h.

An analysis of protein increases of known CRL substrates, with special attention to G2/M regulators, was conducted. Protein extracts were harvested after 4 and 24 h of MLN4924 treatment in order to ensure the specificity and stability of any change detected, respectively (Figure 2a). Specific (already detectable after 4 h of treatment) increases of P27, WEE1, CDC25A and Cyclin E were observed both at medium (IC75) and saturating concentrations (IC95) of the drug and remained constant after 24 h in most of the cell lines. Increases in P21 protein levels were more difficult to detect and were absent in RM82 and TC71. This result was expected as both cell lines are known to lack functional p53¹⁸ and discards any significant contribution of P21 to MLN4924-induced G2/M arrest in ES cell lines. EMI1 (another reported CRL substrate with functions in mitosis regulation) failed to reflect a clear pattern of accumulation.

Increases of CHK1 kinase phosphorylation at Ser345 were also detected, reflecting only mild activation of the DNA damage signaling pathway at medium drug concentrations. More intense activation of this marker was found at higher concentrations (Figure 2a). These observations were validated by γ -H2AX immunofluorescence (Supplementary Figure S3).

Remarkably, only mild increases of CDT1 were observed (Figure 2b). However, CUL1 and CUL4 deneddylation took place in ES cell lines to a similar extent as in HCT116, a colorectal cancer cell line that responds to MLN4924 with dramatic CDT1 increases (Figure 2b) and induced re-replication.^{7,19–20}

Treatment of synchronized ES cells locates MLN4924-induced arrest in G2-early mitosis

RDES cell line was selected to provide a mechanistic insight into MLN4924 action on ES cells. RDES can be synchronized by different methods and responds to MLN4924 treatment with pronounced and stable increases of most of the CRL substrates analyzed.

Synchronization at mitosis with nocodazole, which inhibits the polymerization of microtubules impairing the onset of metaphase,

Table 1. MLN4924 inhibitory concentrations (ICs)

Cell line	1q Copy number	IC50 (nM)	IC75 (nM)	IC95 (nM)
A4573	Gain	60.52 ± 12.20	109.20 ± 15.79	406.28 ± 112.16
A673	Normal	85.00 ± 18.21	148.09 ± 28.64	417.37 ± 185.48
CADOES	Gain	324.91 ± 82.20	467.40 ± 184.56	1009.12 ± 731.96
RDES	Gain	36.80 ± 14.48	77.65 ± 51.54	443.71 ± 238.83
RM82	Gain	73.99 ± 17.90	135.29 ± 24.19	398.77 ± 101.90
SKES	Gain	86.28 ± 14.50	118.20 ± 21.27	240.06 ± 172.04
SKNMC	Normal	52.60 ± 19.58	95.66 ± 27.19	327.59 ± 113.06
STA-ET1	Normal	42.15 ± 11.88	72.87 ± 8.48	189.00 ± 35.39
STA-ET10	Gain	256.73 ± 7.60	430.54 ± 107.43	2579.23 ± 270.45
STA-ET2.1	Normal	103.89 ± 53.22	227.22 ± 59.15	1174.84 ± 615.09
TC32	Gain	152.59 ± 35.11	257.81 ± 63.63	863.85 ± 259.65
TC71	Gain	76.86 ± 2.91	119.13 ± 2.91	265.62 ± 11.82
TTC466	Normal	150.05 ± 2.49	261.99 ± 4.29	735.36 ± 11.65
WE68	Gain	33.02 ± 5.82	85.35 ± 4.54	424.56 ± 106.256

Proliferation ICs of 14 ES cell lines assayed for MLN4924 sensitivity and measured after 72 h exposition to the drug. Mean ± s.d.

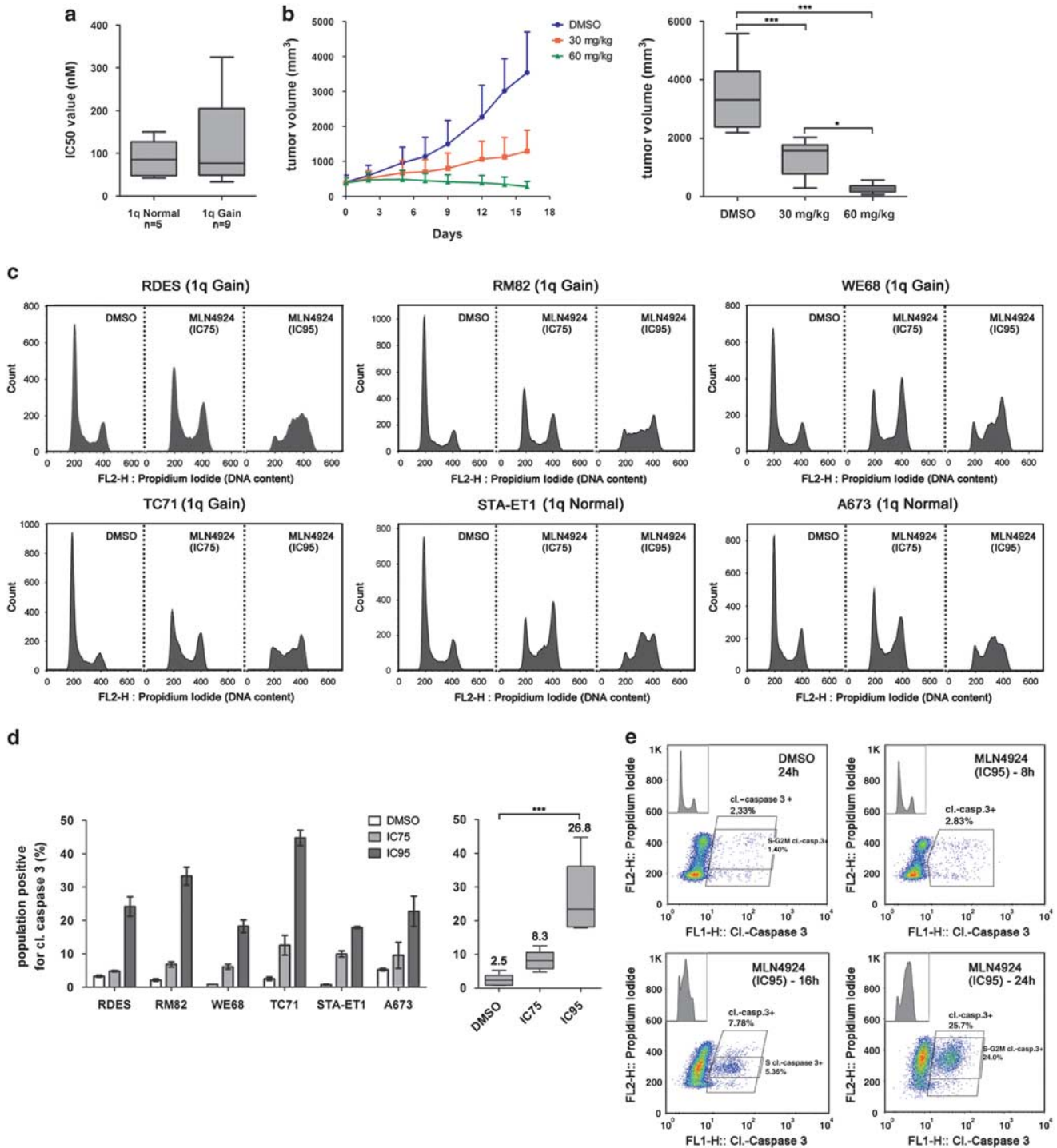


Figure 1. MLN4924 induces G2/M arrest and apoptosis in ES cell lines, which are highly sensitive to this CRL inhibitor. **(a)** No significant differences in IC50 were found between 1q gain and 1q normal ES cell lines. **(b)** Growth of RDES xenografts on mice ($n = 9$ in each treatment condition) was effectively delayed and abolished by 30 mg/kg and 60 mg/kg BID MLN4924 doses, respectively (left panel: evolution of xenograft tumor sizes; right panel: boxplots summarizing final tumor sizes). **(c)** Flow cytometry analysis of DNA content revealed that MLN4924 arrests ES cells in G2/M at low-medium concentrations (FL2-H histograms). SubG1 population was not conspicuous at this time point and was gated out. **(d)** Cleaved Caspase-3 population estimation by flow cytometry showed significant apoptosis triggered at saturating MLN4924 concentrations. Medium doses elicited apoptosis values that only reached marginal significance. Average of two independent replicates. Mean values depicted over the boxplots. **(e)** Combined flow cytometry analysis of Cleaved Caspase-3 and propidium iodide showed an S-phase and S-G2/M DNA content of apoptotic cells after 16 and 24 h, respectively, in IC95 MLN4924-treated RDES cells. Insets: FL2-H (DNA content) histograms. In all cases: mean \pm s.d.; statistical tests: significant analysis of variance, Bonferoni post-hoc test < 0.001 (***) or 0.05 (*).

was used to define more precisely the arrest point within G2/M. After pre-treating RDES cultures with MLN4924 for 4 h (Figure 2c, bottom panel), cells were released from nocodazole and observed

to enter G1 at the same time as control, dimethyl sulfoxide (DMSO) treated cells, discarding any significant contribution of late mitosis CRL substrates to the MLN4924-induced G2/M arrest.

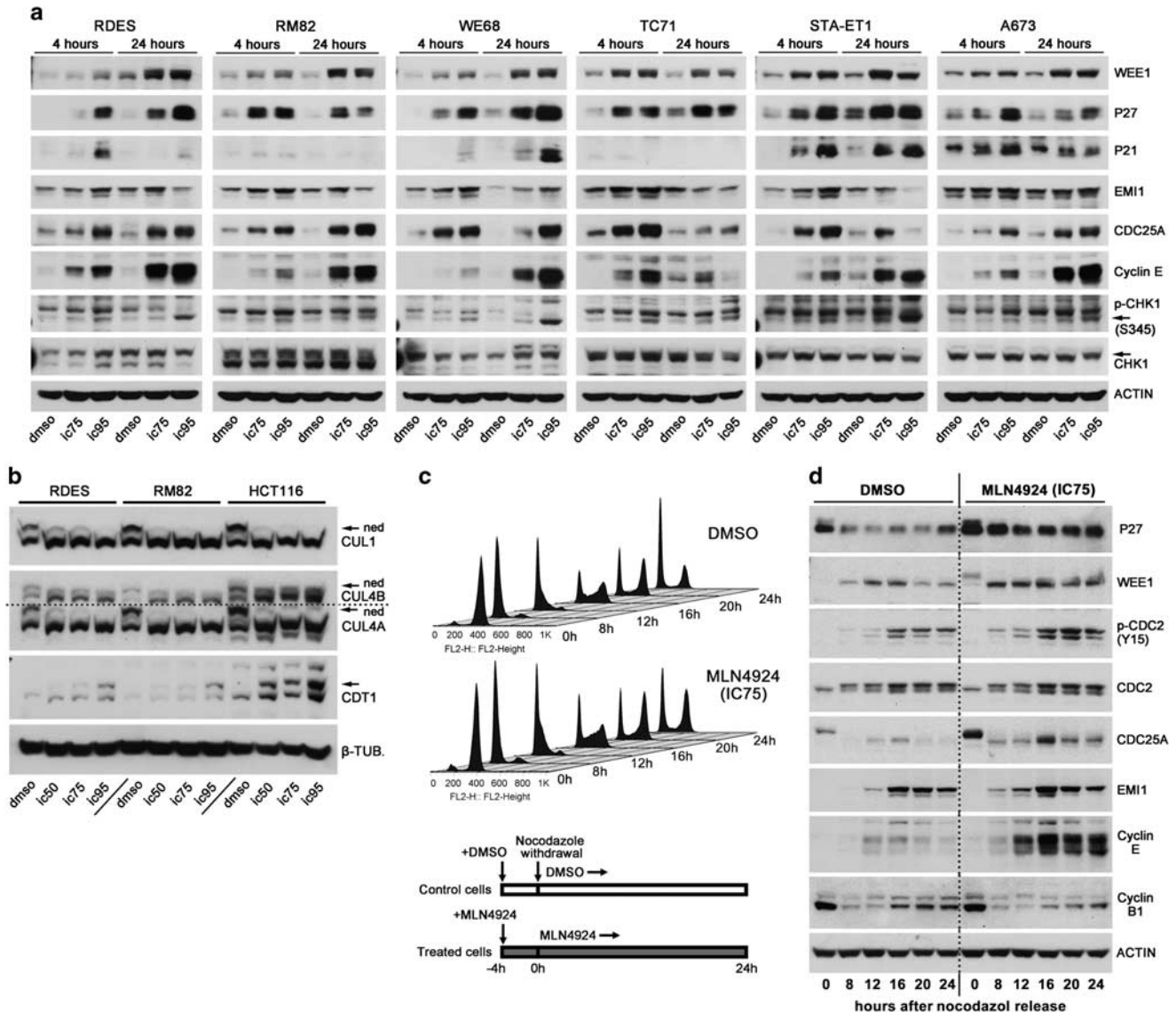


Figure 2. MLN4924 induces protein accumulation of known CRL substrates and arrests RDES cells in G2-early mitosis. **(a)** An analysis of CRL substrates proved the specific and stable accumulation of WEE1, P27, CDC25A and Cyclin E. Arrows: specific bands. **(b)** CDT1 levels increased slightly in ES cells in comparison with HCT116, although deneddylation occurred to a similar extent in both cell types. Arrows: neddylated (ned) cullins. **(c)** Nocodazole-synchronized RDES cells pretreated 4 h with MLN4924 before release were able to enter G1 normally and only showed a significant delay at G2/M (bottom panel: schematic representation of the experiment). **(d)** Accumulated levels of WEE1 and P27 were maintained during all cell cycle stages, in contrast to CDC25A, which decreased in G2/M in spite of CRL inhibition.

In more detail, if late mitosis CRL substrates (expected to be accumulated after MLN4924 pre-treatment) would be implicated in the G2/M arrest, treated cells should show a delayed exit from mitosis and hence MLN4924 should hamper G1 entry after removing nocodazole from the growth medium, which was not observed. In addition, treated cells progressed through undisturbed G1- and S-phases and were only delayed at G2/M (Figure 2c).

Increased WEE1 protein levels were maintained throughout the synchronized cell cycle. Remarkably, a consistent higher phosphorylation of CDC2 (CDK1) at tyrosine 15 (Y15) was also detected, evidencing the functionality of the accumulated WEE1 protein. P27 levels rose from the first time point and were maintained as well (Figure 2d). It is worth noting that CDC25A-induced levels were not constant, peaking at S-phase and decreasing thereafter and seemed to have no effect on cell cycle kinetics. Regarding other substrates analyzed, Cyclin E unscheduled accumulation was detected, whereas EMI1 accumulated only slightly and was present predominantly in mitosis, as expected. Cyclin B1 (a non-

CRL substrate) displayed the normal kinetics in both treated and untreated cells, and was used to monitor progression into mitosis.

Altogether, these results place the MLN4924-induced G2/M arrest in some point before late mitosis and offer two main candidates for a mechanistic explanation: P27 and WEE1.

P27 knockdown and caffeine treatment are unable to revert the G2/M arrest induced by MLN4924

P27 is a CDK inhibitor with a potent regulatory effect over the G1 to S transition. In addition, SCF^{SKP2} CRL complex targets P27 for degradation in late S-G2, rendering an additional role for P27 in the regulation of the G2 to M progression.²¹

We evaluated the ability of P27 knockdown to revert MLN4924-induced G2/M arrest. Despite the substantial P27 decrease obtained by short-hairpin RNA (shRNA) silencing (Figure 3a), no reduction of the population accumulated in G2/M was observed after treating P27-silenced cells with MLN4924 (Figure 3b). Other

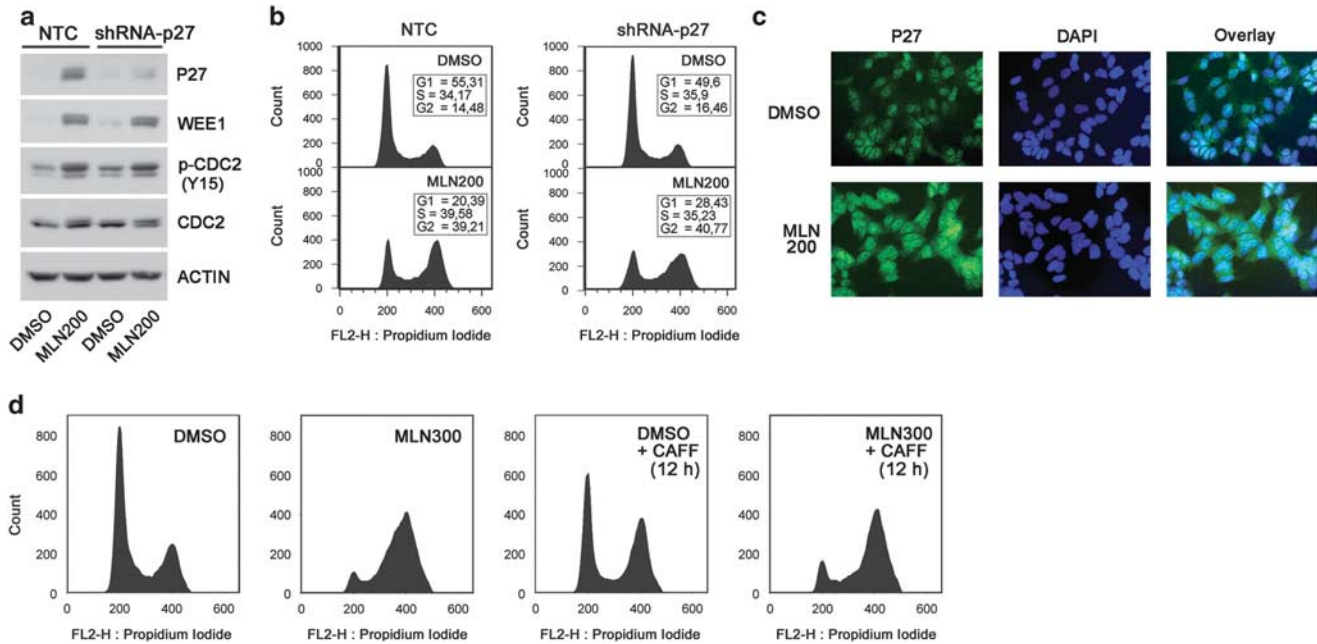


Figure 3. MLN4924-induced G2/M arrest is not reverted by P27 knockdown or caffeine. P27 knockdown efficiently impaired P27 accumulation in treated RDES cells (a) but did not impinge upon the distorted cell cycle distribution caused by MLN4924 (b), despite MLN4924 not showing any effect on P27 subcellular distribution ($\times 20$ magnification immunofluorescence micrographs) (c). Caffeine also failed to affect the G2/M peak (d). P27 knockdown: representative experiment from two independent shRNA cell transductions with similar results. Caffeine was assayed at shorter times with identical results. *caff*, caffeine; MLN200/300, 200/300 nM MLN4924.

shRNA constructions against *P27* yielded similar results (data not shown). Remarkably, P27 knockdown did not affect WEE1 or CDC2-Y15 inhibitory phosphorylation. Silencing of *P27* in RM82 cell line also failed counteracting MLN4924 effects (Supplementary Figure S1A).

Moreover, β -galactosidase assay did not show senescence (a typical effect of p27 accumulation) of RDES cultures treated over 4 days with IC75 drug concentration (data not shown). Surprisingly, MLN4924 did not alter P27 subcellular location, which could have explained the unnoticeable impact of accumulated P27 levels on the cell cycle kinetics of ES cells,²² being most of the protein located inside the nucleus (Figure 3c).

The DNA damage signaling pathway has been previously shown able to arrest the cell cycle in G2.^{23–24} Although only mild CHK1 activation was observed at medium MLN4924 concentrations, we assessed the possible contribution of this signaling pathway to the G2/M arrest. After 24 h of MLN4924 treatment, caffeine (an extensively validated inhibitor of the ATR-ATM DNA damage signaling kinases, here used at a saturating 20 mM concentration) was added to the medium for 12 h. As a result, no noticeable decrease in the MLN4924-induced G2/M peak was observed (Figure 3d).

MLN4924-induced G2/M arrest is reverted by the WEE1 kinase inhibitor PD0166285

WEE1 kinase inhibits the cell cycle progression by phosphorylating CDC2 at Y15, which reduces drastically the enzymatic activity of the CDC2-Cyclin B complex and therefore delays the G2 to M progression.²⁵ Hence, and after having discarded other potential mechanisms, WEE1 role in MLN4924 action on ES cells was inquired.

The WEE1 kinase inhibitor PD0166285 was added to the medium of RDES cultures that had been treated for 21 h with MLN4924 (Figure 4f). PD0166285 treatment was found able to revert the inhibitory phosphorylation of CDC2 at Y15 (Figure 4a)

and to release the cells from the G2/M arrest imposed by MLN4924 (Figure 4b, left panel). Cell cycle quantification showed an increase in G1 population proportional to the G2/M reduction (Figure 4b, right panel). PD0166285 treatment yielded the same results in another cell line (RM82, Supplementary Figure S1B).

Also consistent with a WEE1-imposed G2 arrest, the size of the cell population undergoing mitosis, assessed by flow cytometry analysis of phospho-histone H3-Ser10 (pH3), was found notably reduced by MLN4924 treatment. Most importantly, PD0166285 applied for 1.5 h released MLN4924 G2-arrested cells into mitosis (increasing pH3-positive population from 1 to 18%) and after 3 h the size of the mitotic population reached a value close to that of control cells, indicating the restoration of the normal cell cycle kinetics accomplished by WEE1 inhibition (Figures 4c and d). The anti-pH3 antibody used was confirmed to specifically label mitotic cells and to recognize every stage of mitosis (Supplementary Figure S2 and Figure 4e, respectively).

WEE1 knockdown substantially restores the proliferation and normal cell cycle distribution of MLN4924-treated ES cells.

WEE1 protein levels were depleted to further explore its role mediating MLN4924 action, as PD0166285 could not be maintained in culture at high concentrations and/or long expositions due to toxicity.

Two levels of WEE1 knockdown were obtained by different shRNA constructions with medium (*shwee1-1*) and high (*shwee1-2*) silencing efficiencies, respectively. Each construction reduced CDC2-Y15 phosphorylation in clear correlation with its WEE1 reduction ability (Figure 5a).

Next, *WEE1*-silenced RDES cells were treated with two different MLN4924 concentrations and proliferation was assessed after 48 and 72 h. As a result, both constructions were able to substantially rescue RDES proliferation, with *shwee1-1* being the most efficient (Figure 5b). However, no substantial reduction of apoptosis was

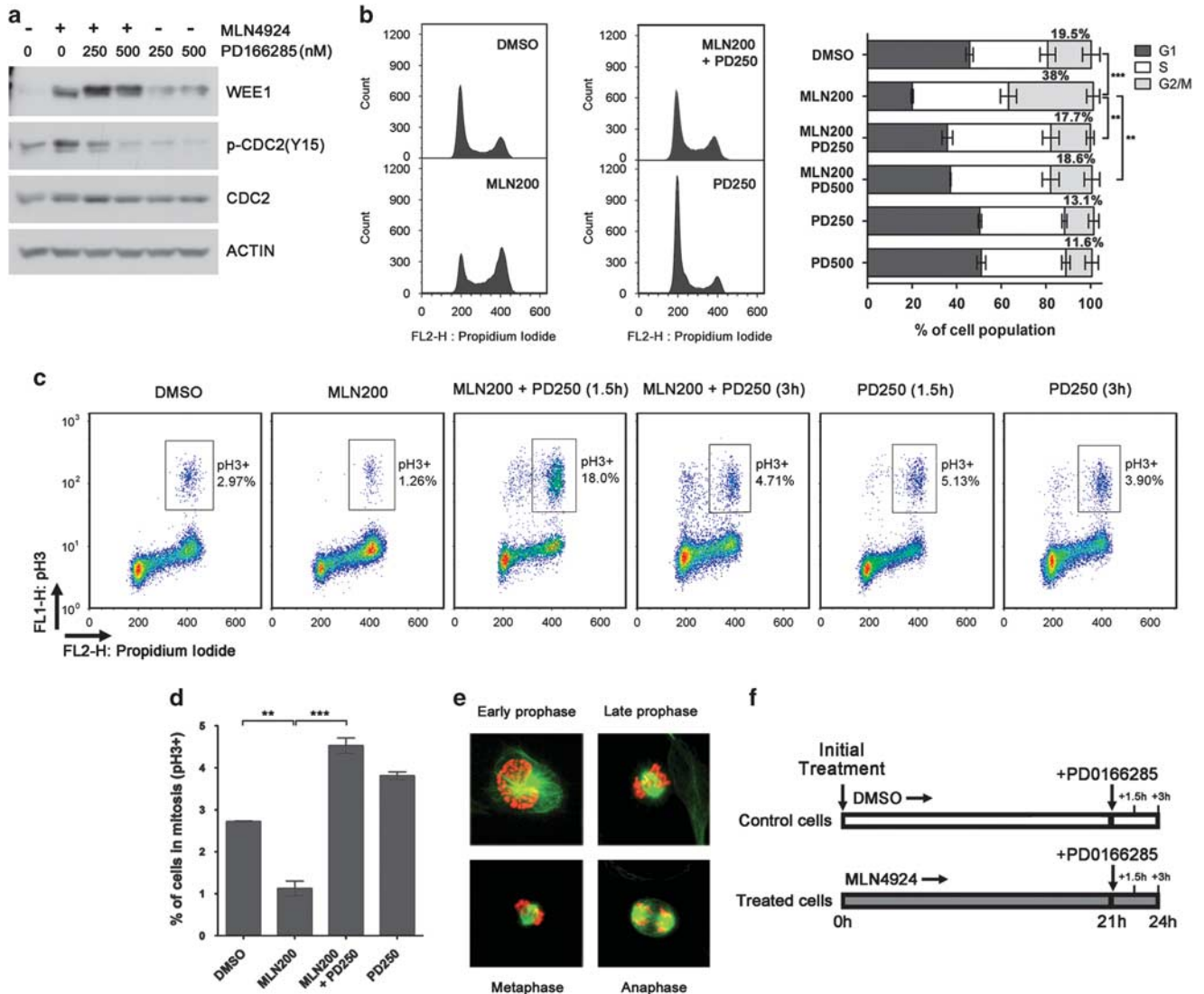


Figure 4. WEE1 inhibition reverts MLN4924-induced G2 arrest. PD0166285 (applied for 3 h to cells arrested by MLN4924 treatment) restored CDC2 phosphorylation at Y15 (a) and G2/M values (b) of MLN4924-treated cells to control levels. (c) MLN4924 was found to reduce the cell population undergoing mitosis (pH3+) whereas PD0166285 restored mitosis (after 1.5 h) and G1 (after 3 h). (d) Quantification of the mitotic population after 3 h of PD0166285 treatment. (e) Immunofluorescence confirmed the specific labeling of mitotic cells by the anti-pH3 antibody used ($\times 40$ magnification micrographs of RDES cells at different mitotic stages: pH3, red; α -tubulin, green). (f) Schematic representation of the experiment. In all cases, mean \pm s.d. of two independent replicates. Statistical tests: significant analysis of variance, Bonferroni post-hoc test < 0.001 (***) and 0.01 (**). MLN200, 200 nM MLN4924; PD250/500, 250 nM/ 500 nM PD0166285.

detected. Indeed, WEE1 knockdown was found to elicit a higher basal (DMSO treatment) cleaved Caspase-3 population labeling when compared with cells transduced with the non-targeting control (NTC). Moreover, WEE1 knockdown-induced apoptosis was proportional to the silencing level achieved by each of the shRNA constructions (Figure 5c). The high value of shwEE1-2-induced apoptosis indicates the dependence of ES cells on WEE1 and explains why this shRNA construction was less efficient in rescuing proliferation despite its better silencing ability.

Finally, both WEE1 shRNA constructions demonstrated a potent effect preventing MLN4924-mediated G2 arrest, although the cell accumulation in S-phase that occurs at saturating concentrations was only partially affected (Figure 5d). The same results were obtained in WEE1-silenced RM82 cells (Supplementary Figure S1C).

Taken together, these results confirm the relevant role of WEE1 in MLN4924 cytostatic effect on ES cell lines, whereas no conclusions can be obtained regarding its contribution to induced

apoptosis as WEE1 depletion triggered apoptosis by itself, probably through mitotic catastrophe.

MLN4924-induced S-phase delay is independent from WEE1 accumulation and simultaneous to depletion and loss of specific functions of CDK2-cyclin A.

WEE1 kinase has been shown to phosphorylate and inhibit CDK2 (the S-phase master regulator) *in vitro*.²⁶ Although the data collected in our previous experiments indicated none or few implication of WEE1 in the S-phase delay detected in MLN4924-treated ES cell lines, we assayed its potential contribution at saturating drug concentrations in synchronically growing RDES cells.

Cells synchronized at the G1-S boundary were MLN4924 pretreated (500 nM) for 2 h before thymidine withdrawal and released in medium with MLN4924 and nocodazole (added to avoid mitotic exit and G1 re-entering; Figure 6e). Treated cells,

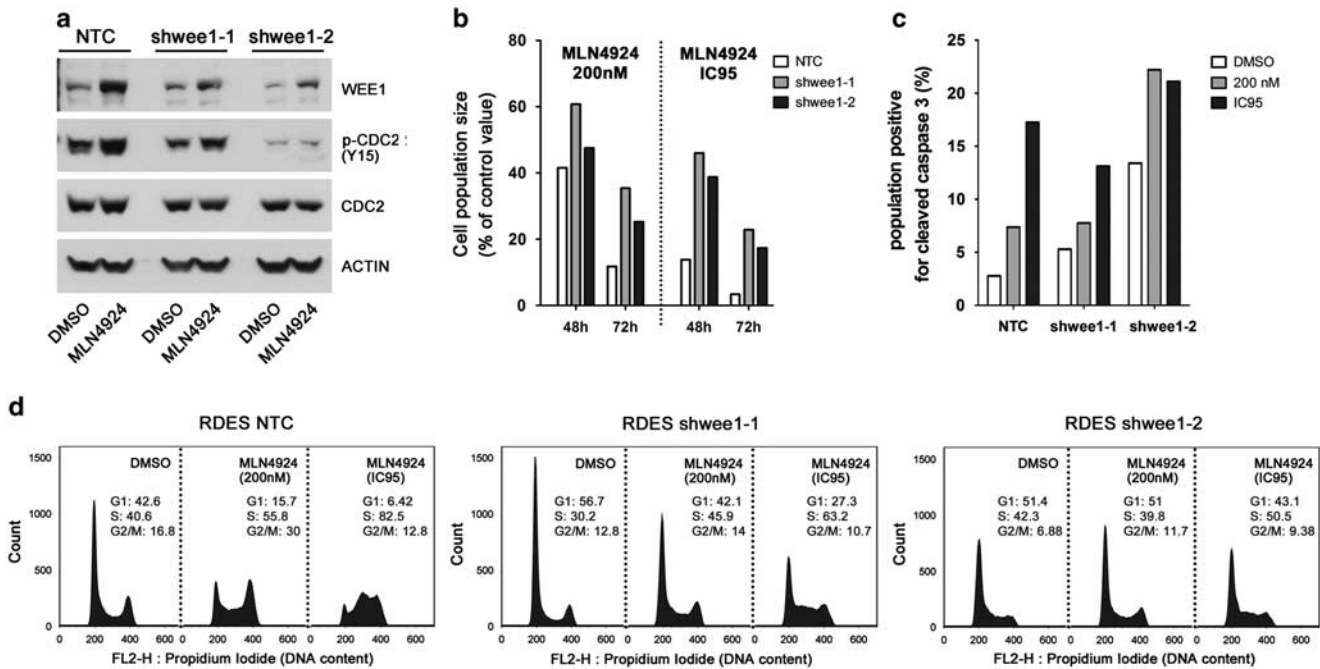


Figure 5. WEE1 knockdown substantially rescues proliferation and prevents MLN4924-induced cell cycle arrest. WEE1 knockdown with two different shRNAs impaired WEE1 protein accumulation after MLN4924 treatment of RDES cells (IC95) and also decreased CDC2-Y15 phosphorylation (a), partially rescuing the proliferation of the cultures at 48 and 72 h (y axis: cell population size of MLN4924-treated cells normalized to control, DMSO treated, values) (b), but was unable to further revert MLN4924 effect on proliferation probably because of the increased basal apoptosis detected in *WEE1*-silenced cells (c). Consistently, flow cytometry analysis revealed a marked effect of WEE1 knockdown preventing the MLN4924-induced G2/M peak (d). Representative experiment from two independent shRNA cell transductions with similar results.

subjected to 5-bromo-2-deoxyuridine (BrdU) pulses, were found to initiate the S-phase in a similar manner to control cells but were severely delayed thereafter (Figure 6a). At 12 h after thymidine withdrawal, a decrease in BrdU incorporation was detected in treated cells (Figure 6b). Consistently, most control cells reached a G2 DNA content at 15 h monitoring time point with few cells still incorporating BrdU, whereas DNA synthesis in MLN4924-treated cells did not progress during the last 6 h, despite BrdU incorporation still taking place. After 24 h, the entire control cell population displayed G2 DNA content whereas treated cells were still delayed and suffering from severe apoptosis (data not shown).

The protein levels of multiple key cell cycle activators and repressors were found dramatically accumulated (Figure 6c). Remarkably, enormous Cyclin E levels were observed during the entire S-phase progression in treated cells while in control cells its levels reduced and disappeared after the S-phase onset (3–6h). Consistently, high increases of pRB (Ser780) were detected at early time points and remained throughout the experiment, evidencing the active enzymatic status of CDK2. In addition, overall levels of Cyclin A were found diminished at the same time points in which treated cells were delayed with respect to control cells.

Immunoprecipitation of CDK2 showed a very slight increase in Y15 phosphorylation, again restricting WEE1 implication in the S-phase delay to few or none (Figure 6d). Strikingly, CDK2 from treated cells co-immunoprecipitated with Cyclin E at time points of advanced S-phase in which CDK2 from control cells did not partner with it, as expected. Conversely, Cyclin A was substantially reduced at the same time points in CDK2 immunoprecipitates of MLN4924-treated cells (Figures 6d and c, respectively), strongly suggesting a displacement of Cyclin A from CDK2 complexes due to Cyclin E saturating protein levels.

CDK2–Cyclin E and CDK2–Cyclin A complexes can impinge different phosphorylation patterns upon CDK2 substrates. One of the best characterized examples of this differential action is CDC6,

which is phosphorylated at S54 and S74 by CDK2–Cyclin E, a modification that is essential for the formation and DNA loading of the pre-replicative complex (pre-RC). Conversely, S106 phosphorylation is specifically exerted by CDK2–Cyclin A and triggers CDC6 relocation to the cytoplasm, a mechanism thought to assure that DNA replication is performed only once per cell cycle.^{27–29}

We used CDC6 subcellular location to confirm the loss of CDK2–Cyclin A-specific functions. As a result, MLN4924-treated cells displayed conspicuous nuclear labeling at late S-phase, 12 hours after thymidine release, whereas CDC6 presence in control ES cells was mainly cytoplasmic, as expected (Figure 6f).

This same assay was carried out with *WEE1*-silenced cells. No significant effect of WEE1 knockdown on the S-phase delay was detected. Caffeine also failed in rescuing the delay under the same experimental conditions (data not shown).

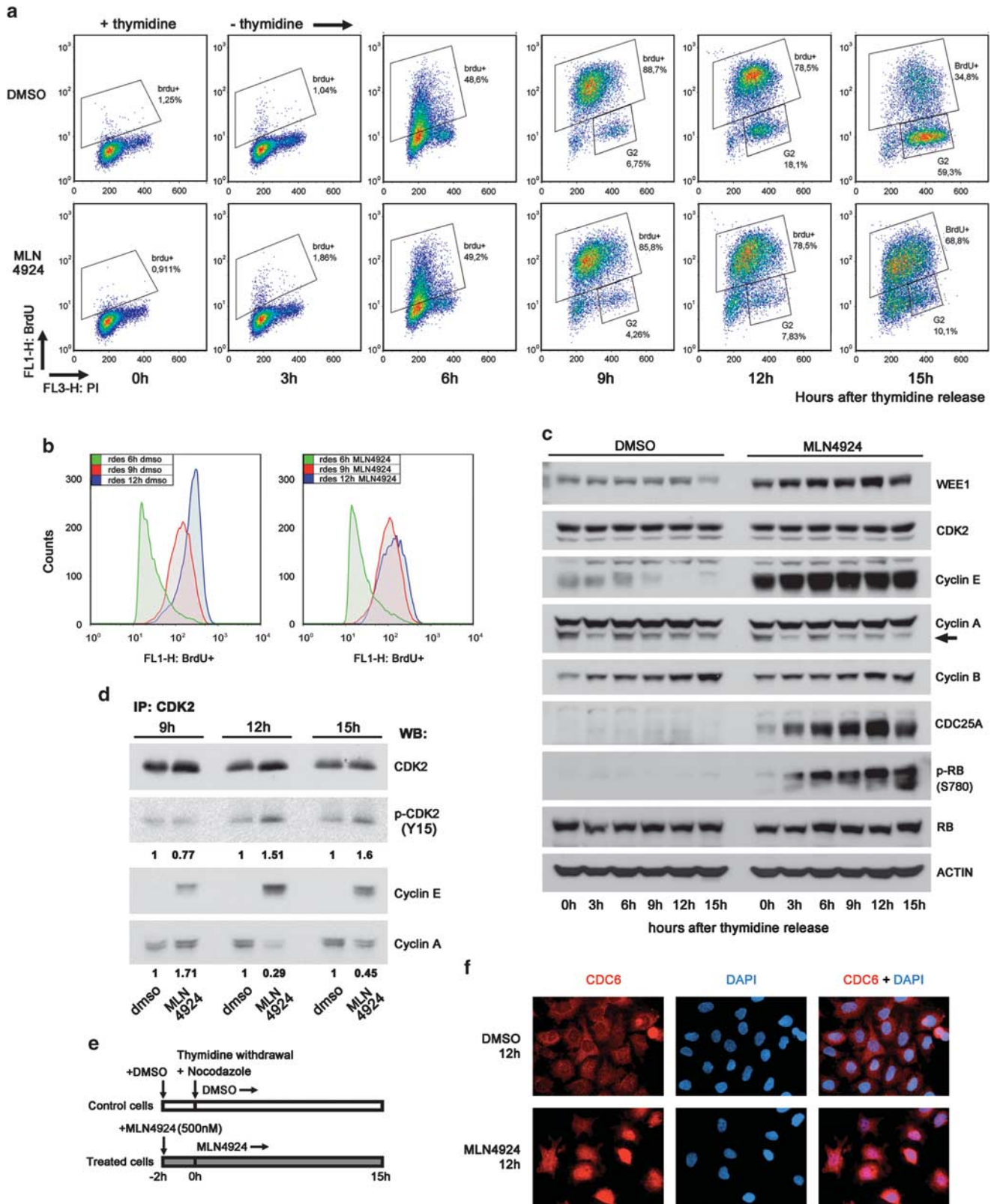
Finally, RDES clones of inducible Cyclin A overexpression were established as an approach to rescue MLN4924-induced late S-phase delay (Supplementary Figure S4A). However, overexpression of Cyclin A was observed to also hamper DNA replication (Supplementary Figure S4B) and thus we could not evaluate its ability to rescue MLN4924-induced S-phase delay. Strikingly, the delay elicited by Cyclin A started in early S-phase, in sharp contrast to the one caused by MLN4924.

DISCUSSION

Here, we report an in-depth preclinical evaluation of MLN4924 in ES. Our results support a potential high sensitivity of this tumor entity to CRL inhibition and render a mechanistic explanation for its activity in ES cells, revealing WEE1 accumulation as a major effector of MLN4924 potent cytostatic activity. In addition, our data suggest that the induced G2 arrest could also be involved in MLN4924 cytotoxic action (Figure 1e). The contribution of other mechanisms, prevalent at saturating concentrations, was also

explored. The evidences shown here point to CDK2-Cyclin A depletion as the most probable cause of the singular effect observed on S-phase, characterized by a huge CDK2 enzymatic activity (as proved by both the phosphorylated status of RB and

the incorporation of BrdU) without completion of DNA synthesis. Consistent with this idea, aberrant location of CDC6 in the nucleus was detected in MLN4924-treated cells in late S-phase, confirming the loss of CDK2-cyclin A-specific functions.



A previous study has evaluated the sensitivity of a set of pediatric tumors to MLN4924, including 6 ES cell lines, although not providing any further insight into the mechanism of action elicited.¹⁷ In this work, in spite of the acute *in vitro* response of ES cells to MLN4924 (the most sensitive among those tested), the treatment of tumors xenografted in mice was not found to induce any significant reduction in tumor size, an observation that was not restricted to ES cells but that affected most malignant cell types assayed. Apart from this internal inconsistency, the lack of *in vivo* effects in ES cells is in clear contrast with our data, especially when taking into account that the doses found effective *in vivo* in our study are considerably lower than those described in the said article. Remarkably, the authors mentioned that such high doses of the compound gave rise to a skin-hardening problem at the site of injection that led to a premature interruption of the assay. So, a suboptimal uptake of the drug due to this impediment might underlie the discrepancy between both studies.

Strikingly, MLN4924 arrests ES cells in G2 in sharp contrast with CDT2 knockdown, which halted the cells in G1,³ and in accordance with the similar sensitivity and response of 1q gain and 1q normal ES cell lines to the said compound. Having discarded a molecular mechanism specific of 1q gain ES, the model proposed here could find a broader application not only to virtually all ES tumors but also to other tumor types that respond to MLN4924 treatment with G2 arrest/S-phase delay. In addition, this mechanism is triggered by a wide range of drug concentrations in cell culture, including levels easily attainable by *in vivo* dosing (< 100 nm).

The protein levels of CDT1, a substrate of both CUL4/DDB1^{CDT2} and SCF^{SKP2} CRL complexes,³⁰ were only slightly affected by MLN4924 in ES cells compared with HCT116. Consistently, the response of each of these cell types to CRL inhibition differs greatly.^{7,19} However, deneddylation of CUL4 and CUL1 took place in ES cell lines to the same extent as in HCT116 (Figure 2b). These clearly dissimilar responses to CRL inhibition are not surprising as it is already known that despite the great selectivity of MLN4924 for its specific target UBA3⁷ its potent antitumoral action is exerted by different mechanisms depending on the cellular background,^{16,19–20,31–32} probably due to intercellular differences in the configuration of CRL substrates and CRL components and to cell-type-specific ubiquitinomes.^{5,33} Most importantly, this phenomenon raises a relevant concern: the precise characterization of MLN4924 molecular mechanisms in each different malignant cell type is imperative for a better understanding of its clinical applications. Regarding this matter, a phase I clinical trial of MLN4924 in advanced nonhematologic malignancies is ongoing in the United States (ClinicalTrials.gov NCT00677170).

Besides, this report points out another interesting finding: the accumulation of some particular CRL substrates as a consequence of CRL inhibition might carry no functional manifestation in specific types of transformed cells. The results of the assays concerning P27 role in MLN4924 response suggest this conclusion. Also supporting this idea, it has been recently shown how several kinases (ABL, LYN and SRC) phosphorylate P27 at Tyr88 and Tyr74 during G1 to S transition and how these phosphorylations cause the ejection of P27 from the catalytic cleft of the Cyclin E–CDK2 complexes, being a prerequisite for the phosphorylation at Thr187

exerted by Cyclin E–CDK2 itself.^{34–36} Phosphorylation at Thr187 is the mark that enables recognition of P27 by the SCF complex and is the starting point for its ubiquitination and degradation.³⁷ Therefore, MLN4924 could be inducing the accumulation of an inactive P27 form, which might explain why this tumor suppressor does not seem to have any significant role in MLN4924 effects on ES cells, despite its nuclear localization. In line with this idea, CDC25A and Cyclin E combined accumulation is expected to induce a premature entry in G1,³⁸ which was not observed neither in nocodazole nor in thymidine-synchronized ES cells subjected to MLN4924 treatment. Moreover, CDC25A did not seem to have any effect on accelerating G2 to M progression either. So, both results suggest an also absence of function of the CDC25A protein accumulated in response to MLN4924 treatment. This point was not further explored as it has no relevance for the aims pursued in this study.

Alternatively, the ultimate effect of CRL inhibition could be the result of the net balance of opposed and/or overlapped deregulated protein activities, whose final outcome would be conditioned by the different, cell-type-dependent proteome and interactome configurations. According to this idea, WEE1 accumulation would represent the 'prevailing force' in ES cells subjected to CRL inhibition. However, the results reported in this study favor the hypothesis expressed in the former paragraph.

Finally, WEE1 provides an important advantage when considered as a therapeutic effector, as WEE1 loss drives the cells into mitotic catastrophe and, subsequently, into apoptosis.³⁹ Hence, tumor cells could difficultly develop resistance by losing WEE1 function, in contrast to what could be expected of any therapy relying on other effectors frequently found lost in cancer such as P21 and P27. *WEE1* is a ubiquitously expressed gene, key regulator of the cell cycle, and thus WEE1 is present in virtually any malignant cell that could be considered as potentially treatable with this or similar compounds. In addition, WEE1 has recently been implicated in the radiosensitization of two human pancreatic cancer cell lines by MLN4924.⁴⁰ So, WEE1 accumulation could be of further clinical use by empowering other antitumoral therapies. Regarding this issue, ongoing work in our laboratories is exploring the best drug combinations aiming an eventual inclusion of MLN4924 into traditional ES treatment schemes.

We have thus reported how MLN4924 inhibits ES cell growth and how its potent cytostatic effect depends on WEE1 accumulation.

MATERIALS AND METHODS

Cell lines and pharmaceutical compounds

A4573, A673, CADO-ES, RDES, RM82, SKES, SKNMC, STAET-1, STAET-2.1, STAET-10, TC71, TTC466, TC32 and WE68 were obtained from the EuroBoNet cell line panel that is maintained and regularly checked and characterized by Ottaviano *et al.*⁴¹ in Heinrich-Heine-University at Düsseldorf, by the methods explained in reference. Cells were grown on gelatin-coated plates in RPMI 10–20% except for A673 (DMEM 10%).

MLN4924 was provided by Millennium Pharmaceuticals, Inc. (The Takeda Oncology Company, Cambridge, MA, USA). PD0166285 was purchased from Tocris Bioscience (Ellisville, MO, USA). Both were dissolved in DMSO for *in vitro* assays.

Figure 6. High MLN4924 concentrations cause a severe S-phase delay independent from WEE1 accumulation. Synchronized RDES cells were BrdU-pulsed and analyzed by flow cytometry (a) revealing a decrease in BrdU incorporation detectable 12 h after thymidine withdrawal (FL1-H histograms of the populations gated in A, BrdU+) (b). Western blot of protein extracts at each monitoring time showed unscheduled presence of enormous Cyclin E amounts at late S-phase, correlating with diminished Cyclin A levels and huge phosphorylation of RB at Ser780 (arrow: Cyclin A-specific band) (c). CDK2 immunoprecipitation showed slight increase of CDK2-Y15 phosphorylation and aberrant co-immunoprecipitation of Cyclin E at late S time points. Cyclin A presence in the same immunoprecipitates was heavily reduced (d). Schematic representation of the experiment (e). Immunofluorescence study of CDC6 subcellular location revealed aberrant nuclear staining in cells subjected to MLN4924 treatment (f). Numbers below p-CDK2-Y15 and Cyclin A blots represent densitometric quantifications of MLN4924 bands, normalized to CDK2 and referred to their respective controls (DMSO band from the same time point). Representative experiment from several independent synchronization assays. PI: propidium iodide.

Cell viability assay

Cells were seeded at 3000–4000 per well in 96-well culture plates. MLN4924 was added to complete growth medium at concentrations ranging from 0.001 to 10 μ M. After 72 h, cells were subjected to the ATPlite assay (PerkinElmer, Waltham, MA, USA) and inhibitory concentrations were calculated.

Tumor xenografts in mice

RDES cells were trypsinized and counted. Suspensions containing 4×10^6 living cells in a 0.2 ml final volume composed of RPMI medium and Matrigel Matrix (Becton Dickinson, Franklin Lakes, NJ, USA) in a 1:1 proportion were injected subcutaneously in five-week-old CB.17 SCID female mice (Harlan, Indianapolis, IN, USA). Tumor size was measured with a caliper, and treatment was started when the mean volume reached 400 mm³. Animals were dosed subcutaneously with vehicle (10% β -cyclodextrin) or MLN4924. At 16 days after injection, tumor volumes reached tolerable size limits and animals were euthanized by anesthetic overdose. All animals were housed and handled in accordance with the Guide for the Care and Use of Laboratory Animals, and the study was previously approved by the Bioethics Committee of the University of Salamanca.

PH3, P27 and CDC6 immunofluorescence

Cells were grown in gelatin-coated 6 cm plates, fixed with 3.6% paraformaldehyde for 8 min and permeabilized with ice-cold methanol applied for 3 min. After phosphate-buffered saline (PBS) rehydration and washes, plates were blocked with 1% BSA in PBS and incubated overnight at 4 °C with 1:1000 anti-pH3 antibody (Cell Signalling, Danvers, MA, USA) and 1:500 anti- α -tubulin (Calbiochem, Merck KGaA, Darmstadt, Germany) or 1:500 anti-P27 (BD, Franklin Lakes, NJ, USA) or 1:50 anti-CDC6 (Santa Cruz Biotechnology, Santa Cruz, CA, USA) under coverslips and inside humidified petri dishes. Cy3- (Jackson ImmunoResearch Laboratories, West Grove, PA, USA) and Alexa Fluor 488-labeled secondary antibodies (Invitrogen, Carlsbad, CA, USA) were applied under coverslips and incubated 1 h at room temperature. Finally, DAPI was added for 2 min to counterstain DNA.

Additional methods are described in Supplementary Material and Methods.

CONFLICT OF INTEREST

Peter G Smith was an employee of Millennium Pharmaceuticals, Inc. at the time of this study. There are no other competing financial interests.

ACKNOWLEDGEMENTS

We thank Cristina Teodosio and Martín Pérez de Andrés for their kind help in flow cytometry studies. Daniel J García-Domínguez is supported by a grant from the María García Estrada Foundation. Research in Enrique de Alava's lab is also supported by the Ministry of Economy and Competitiveness of Spain-FEDER (PI081828, RD06/0020/0059, PI1100018, ISCIII_postdoc grant CD06/00001) and the European Commission (FP7-HEALTH-2011-two-stage, Project ID 278742 EUROSARC).

Author contributions: CM conceived the study and its design, analyzed the data and wrote the manuscript. The experimental work was accomplished by CM and DJGD. DJGD and JLO carried out the work with animals. AGP, PGS, MPS and EDA participated in conceptualization of the study and in critical discussion of data. All authors revised and edited the manuscript.

REFERENCES

- Bernstein M, Kovar H, Paulussen M, Randall RL, Schuck A, Teot LA *et al*. Ewing's sarcoma family of tumors: current management. *Oncologist* 2006; **11**: 503–519.
- Haeusler J, Ranft A, Boelling T, Goshager G, Braun-Munzinger G, Vieth V *et al*. The value of local treatment in patients with primary, disseminated, multifocal Ewing sarcoma (PDMES). *Cancer* 2010; **116**: 443–450.
- Mackintosh C, Ordonez JL, Garcia-Dominguez DJ, Sevillano V, Llombart-Bosch A, Szuhaï K *et al*. 1q gain and CDT2 overexpression underlie an aggressive and highly proliferative form of Ewing sarcoma. *Oncogene* 2012; **31**: 1287–1298.
- Cardozo T, Pagano M. The SCF ubiquitin ligase: insights into a molecular machine. *Nat Rev Mol Cell Biol* 2004; **5**: 739–751.
- Bennett EJ, Rush J, Gygi SP, Harper JW. Dynamics of cullin-RING ubiquitin ligase network revealed by systematic quantitative proteomics. *Cell* 2010; **143**: 951–965.

- Frescas D, Pagano M. Deregulated proteolysis by the F-box proteins SKP2 and beta-TrCP: tipping the scales of cancer. *Nat Rev Cancer* 2008; **8**: 438–449.
- Soucy TA, Smith PG, Milhollen MA, Berger AJ, Gavin JM, Adhikari S *et al*. An inhibitor of NEDD8-activating enzyme as a new approach to treat cancer. *Nature* 2009; **458**: 732–736.
- Duda DM, Borg LA, Scott DC, Hunt HW, Hammel M, Schulman BA *et al*. Structural insights into NEDD8 activation of cullin-RING ligases: conformational control of conjugation. *Cell* 2008; **134**: 995–1006.
- Liao H, Liu XJ, Blank JL, Bouck DC, Bernard H, Garcia K *et al*. Quantitative proteomic analysis of cellular protein modulation upon inhibition of the NEDD8-activating enzyme by MLN4924. *Mol Cell Proteomics*. (e-pub ahead of print 2011; doi:10.1074/mcp.M111.009183).
- Carrano AC, Eytan E, Hershko A, Pagano M. SKP2 is required for ubiquitin-mediated degradation of the CDK inhibitor p27. *Nat Cell Biol* 1999; **1**: 193–199.
- Yu ZK, Gervais JL, Zhang H. Human CUL-1 associates with the SKP1/SKP2 complex and regulates p21(CIP1/WAF1) and cyclin D proteins. *Proc Natl Acad Sci USA* 1998; **95**: 11324–11329.
- Tan P, Fuchs SY, Chen A, Wu K, Gomez C, Ronai Z *et al*. Recruitment of a ROC1-CUL1 ubiquitin ligase by Skp1 and HOS to catalyze the ubiquitination of I kappa B alpha. *Mol Cell* 1999; **3**: 527–533.
- Watanabe N, Arai H, Nishihara Y, Taniguchi M, Hunter T, Osada H. M-phase kinases induce phospho-dependent ubiquitination of somatic Wee1 by SCFbeta-TrCP. *Proc Natl Acad Sci USA* 2004; **101**: 4419–4424.
- Busino L, Donzelli M, Chiesa M, Guardavaccaro D, Ganoth D, Dorrello NV *et al*. Degradation of Cdc25A by beta-TrCP during S phase and in response to DNA damage. *Nature* 2003; **426**: 87–91.
- Singer JD, Gurian-West M, Clurman B, Roberts JM. Cullin-3 targets cyclin E for ubiquitination and controls S phase in mammalian cells. *Genes Dev* 1999; **13**: 2375–2387.
- Milhollen MA, Traore T, Adams-Duffy J, Thomas MP, Berger AJ, Dang L *et al*. MLN4924, a NEDD8-activating enzyme inhibitor, is active in diffuse large B-cell lymphoma models: rationale for treatment of NF-(kappa)B-dependent lymphoma. *Blood* 2010; **116**: 1515–1523.
- Smith MA, Maris JM, Gorlick R, Kolb EA, Lock R, Carol H *et al*. Initial testing of the investigational NEDD8-activating enzyme inhibitor MLN4924 by the pediatric preclinical testing program. *Pediatr Blood Cancer* (e-pub ahead of print 2011; doi: 10.1002/pbc.23357).
- Ottaviano L, Schaefer KL, Gajewski M, Huckenbeck W, Baldus S, Rogel U *et al*. Molecular characterization of commonly used cell lines for bone tumor research: a trans-European EuroBoNet effort. *Genes Chromosomes Cancer* 2010; **49**: 40–51.
- Lin JJ, Milhollen MA, Smith PG, Narayanan U, Dutta A. NEDD8-targeting drug MLN4924 elicits DNA rereplication by stabilizing Cdt1 in S phase, triggering checkpoint activation, apoptosis, and senescence in cancer cells. *Cancer Res* 2010; **70**: 10310–10320.
- Milhollen MA, Narayanan U, Soucy TA, Veiby PO, Smith PG, Amidon B *et al*. Inhibition of NEDD8-activating enzyme induces rereplication and apoptosis in human tumor cells consistent with deregulating CDT1 turnover. *Cancer Res* 2011; **71**: 3042–3051.
- Nakayama K, Nagahama H, Minamishima YA, Miyake S, Ishida N, Hatakeyama S *et al*. Skp2-mediated degradation of p27 regulates progression into mitosis. *Dev Cell* 2004; **6**: 661–672.
- Susaki E, Nakayama KI. Multiple mechanisms for p27(Kip1) translocation and degradation. *Cell Cycle* 2007; **6**: 3015–3020.
- Syljuasen RG, Jensen S, Bartek J, Lukas J. Adaptation to the ionizing radiation-induced G2 checkpoint occurs in human cells and depends on checkpoint kinase 1 and Polo-like kinase 1 kinases. *Cancer Res* 2006; **66**: 10253–10257.
- Bartek J, Lukas J. Chk1 and Chk2 kinases in checkpoint control and cancer. *Cancer Cell* 2003; **3**: 421–429.
- McGowan CH, Russell P. Human Wee1 kinase inhibits cell division by phosphorylating p34cdc2 exclusively on Tyr15. *EMBO J* 1993; **12**: 75–85.
- Watanabe N, Broome M, Hunter T. Regulation of the human WEE1Hu CDK tyrosine 15-kinase during the cell cycle. *EMBO J* 1995; **14**: 1878–1891.
- Jiang W, Wells NJ, Hunter T. Multistep regulation of DNA replication by Cdk phosphorylation of HsCdc6. *Proc Natl Acad Sci USA* 1999; **96**: 6193–6198.
- Petersen BO, Lukas J, Sorensen CS, Bartek J, Helin K. Phosphorylation of mammalian CDC6 by cyclin A/CDK2 regulates its subcellular localization. *EMBO J* 1999; **18**: 396–410.
- Paolinelli R, Mendoza-Maldonado R, Cereseto A, Giacca M. Acetylation by GCN5 regulates CDC6 phosphorylation in the S phase of the cell cycle. *Nat Struct Mol Biol* 2009; **16**: 412–420.
- Nishitani H, Sugimoto N, Roukos V, Nakanishi Y, Saijo M, Obuse C *et al*. Two E3 ubiquitin ligases, SCF-Skp2 and DDB1-Cul4, target human Cdt1 for proteolysis. *EMBO J* 2006; **25**: 1126–1136.

- 31 Swords RT, Kelly KR, Smith PG, Garnsey JJ, Mahalingam D, Medina E *et al*. Inhibition of NEDD8-activating enzyme: a novel approach for the treatment of acute myeloid leukemia. *Blood* 2010; **115**: 3796–3800.
- 32 Jia L, Li H, Sun Y. Induction of p21-dependent senescence by an NAE inhibitor, MLN4924, as a mechanism of growth suppression. *Neoplasia* 2011; **13**: 561–569.
- 33 Kim W, Bennett EJ, Huttlin EL, Guo A, Li J, Possemato A *et al*. Systematic and quantitative assessment of the ubiquitin-modified proteome. *Mol Cell* 2011; **44**: 325–340.
- 34 Grimmer M, Wang Y, Mund T, Cilensek Z, Keidel EM, Waddell MB *et al*. Cdk-inhibitory activity and stability of p27Kip1 are directly regulated by oncogenic tyrosine kinases. *Cell* 2007; **128**: 269–280.
- 35 Chu I, Sun J, Arnaout A, Kahn H, Hanna W, Narod S *et al*. p27 phosphorylation by Src regulates inhibition of cyclin E-Cdk2. *Cell* 2007; **128**: 281–294.
- 36 Russo AA, Jeffrey PD, Patten AK, Massague J, Pavletich NP *et al*. Crystal structure of the p27Kip1 cyclin-dependent-kinase inhibitor bound to the cyclin A-Cdk2 complex. *Nature* 1996; **382**: 325–331.
- 37 Tsvetkov LM, Yeh KH, Lee SJ, Sun H, Zhang H. p27(Kip1) ubiquitination and degradation is regulated by the SCF(Skp2) complex through phosphorylated Thr187 in p27. *Curr Biol* 1999; **9**: 661–664.
- 38 Vigo E, Muller H, Prosperini E, Hateboer G, Cartwright P, Moroni MC *et al*. CDC25A phosphatase is a target of E2F and is required for efficient E2F-induced S phase. *Mol Cell Biol* 1999; **19**: 6379–6395.
- 39 Mir SE, De Witt Hamer PC, Krawczyk PM, Balaj L, Claes A, Niers JM *et al*. In silico analysis of kinase expression identifies WEE1 as a gatekeeper against mitotic catastrophe in glioblastoma. *Cancer Cell* 2010; **18**: 244–257.
- 40 Wei D, Li H, Yu J, Sebolt JT, Zhao L, Lawrence TS *et al*. Radiosensitization of human pancreatic cancer cells by MLN4924, an investigational NEDD8-activating enzyme inhibitor. *Cancer Res* 2012; **72**: 282–293.
- 41 Ottaviano L, Schaefer KL, Gajewski M, Huckenbeck W, Baldus S, Rogel U *et al*. Molecular characterization of commonly used cell lines for bone tumor research: a trans-European EuroBoNet effort. *Genes Chromosomes Cancer* 2010; **49**: 40–51.

Supplementary Information accompanies the paper on the Oncogene website (<http://www.nature.com/onc>)